

The Evaluation of Cryogenic Force Balance Calibration Methodologies with Respect to Wind Tunnel Results

Devin E. Burns ^{*}, Kenneth G. Toro [†], Peter A. Parker [‡], and S. Melissa Rivers [§]

NASA Langley Research Center, Hampton, Virginia, 23681, USA

Harald Quix [¶], and Martin Wright ^{||}

European Transonic Windtunnel, Köln, 51147, Germany

Independent tests of the NASA Common Research Model (CRM) at NASA’s National Transonic Facility (NTF) and the European Transonic Windtunnel (ETW) revealed discrepancies at low operating temperatures and high Reynolds numbers that warranted further investigation. Since each facility used their own force balance for their tunnel entry, one suggestion for the discrepancy was the temperature compensation methodology developed and applied for each balance. This hypothesis is explored through simulation and experimentally. Independent calibrations of NASA’s NTF-118A balance at NASA Langley and ETW reveal discrepancies in the thermal compensation of the normal force and pitching moment primary sensitivities with temperature, while the axial force primary sensitivities are in good agreement. The application of the force balance calibrations performed at NASA and ETW to the prior wind tunnel data suggests that the thermal compensation discrepancies are an order of magnitude less than the discrepancies observed between the wind tunnel aerodynamic coefficients.

Nomenclature

- BCM Balance Calibration Machine
- CRM Common Research Model
- ETW European Transonic Windtunnel
- NASA National Aeronautics and Space Administration
- NTF National Transonic Facility
- RTD Resistance Temperature Detector
- SC Temperature Sensitivity Constant

I. Introduction

The NASA Common Research Model (CRM)¹ is a transport style aircraft wind tunnel model developed to provide a publicly available experimental database that can be used to validate computational fluid dynamics simulations. The CRM has also been tested at wind tunnel facilities around the world allowing facilities to benchmark their results to a common wind tunnel model. Among these tests, the CRM was tested at both of the cryogenic wind tunnels in the world — NASA’s National Transonic Facility (NTF) and the European Transonic Windtunnel (ETW).

Entries of the CRM at NTF and ETW relied on each tunnel to provide their own model support hardware and instrumentation including wind tunnel force balances and angle measurement systems. The NTF used

^{*}Balance Engineer, Advanced Measurement and Data Systems, NASA Langley Research Center

[†]Research Engineer, System Engineering and Engineering Methods, NASA Langley Research Center

[‡]Team Lead, Advanced Measurement and Data Systems, NASA Langley Research Center

[§]Research Engineer, Configuration Aerodynamics Branch, NASA Langley Research Center

[¶]Group Leader Test and Data Systems Group, European Transonic Windtunnel

^{||}Manager Aerodynamics and Testing, European Transonic Windtunnel

NASA Langley’s NTF-118A wind tunnel force balance for the CRM entry, while ETW used its’ B004 wind tunnel force balance. Each of these wind tunnel force balances was independently calibrated at NASA and ETW, respectively.

Wind tunnel results at near ambient temperature (301 K) and Reynolds number of 5×10^6 showed good agreement between the facilities. However, at low temperatures (116 K) and high Reynolds numbers in excess of 19.8×10^6 an offset between the coefficient of lift and the pitching moment coefficient curves was observed outside of tolerance limits.² One potential hypothesis for the discrepancy was the thermal compensation algorithms derived from the balance calibrations.

This work explores several aspects of this claim. First, the methodologies and processes for cryogenic calibration of force balances are explained for both NASA and ETW. Second, a simulation is performed to assess the extent of error due to the balance temperature effects that would be required to reconcile the ETW and NTF data. Next, independent calibrations of NASA’s NTF-118A force balance are performed at NASA and ETW. The calibration data are used to determine the extent of temperature related differences in the calibration and their effect on the wind tunnel data.

II. Room Temperature Calibration

Room temperature calibration procedure and hardware forms the basis for cryogenic calibration. This section outlines the calibration and data reduction methods used at ETW and NASA.

II.A. ETW’s Approach

At ETW, there are only minor differences between the room temperature and cryogenic calibration procedure. All calibrations are performed using ETW’s fully automated Balance Calibration Machine (BCM).^{3,4} The BCM was designed and built to calibrate ETW’s cryogenic balances over the complete temperature range of ETW and it is presently the only, automated cryogenic force balance calibration system in the world. At all temperatures the BCM can achieve the following maximum loads:

Load Component	BCM Load Limits
F _x	± 2300 N
F _y	± 3000 N
F _z	± 25000 N
M _x	± 850 Nm
M _y	± 1300 Nm
M _z	± 500 Nm

Table 1. BCM load limits.

The concept of the BCM is based on loading by pneumatic force generators. The applied loads are measured simultaneously by six master load cells (forming the external reference balance) and by the wind tunnel balance, hereafter called the internal balance. The master loads cells are mounted on the measurement frame, colored orange in Figure 1, while the force generators are connected to the loading frame, colored light gray in Figure 1. The measurement frame and the loading frame are connected by the internal balance which is mounted with its live (metric) side to the measurement frame to keep the external and internal balance coordinate systems load independent. The internal balance earth (non-metric, ground) side is connected to the loading frame via a flange, so that deflections on this side due to loadings can be neglected.

The area around the internal balance, between the measurement frame flange and the loading tree flange, is covered by a temperature controlled housing. This cryogenic calibration chamber allows temperature changes of the internal balance over the full operating envelope of ETW, while the external balance is well insulated and kept at ambient temperature.

For standard room temperature calibrations the calibration chamber is left open, so that the temperatures of the internal balance as well as the external balance are controlled by the calibration room air conditioning system. The calibration runs fully automated applying the loads of a predefined load schedule. These

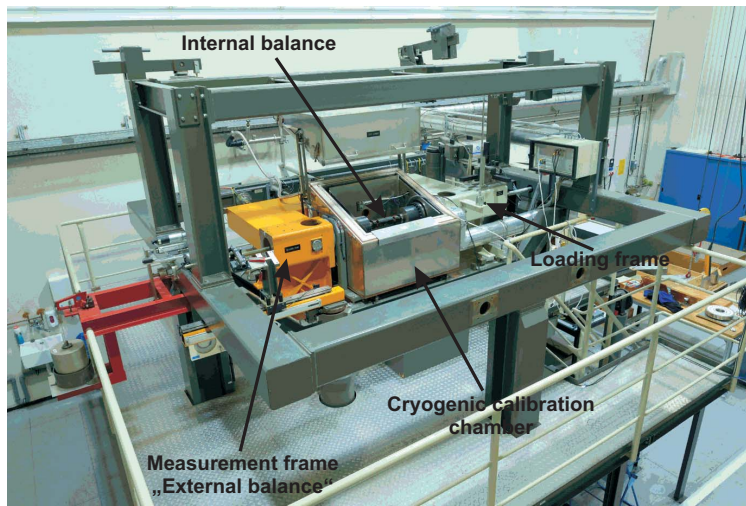


Figure 1. Schematic view of BCM.

predefined loads are input parameters to the BCM control software, which will convert the required loads into pressures supplied by the pneumatic force generators. Because the applied loads are accurately measured by the external balance, no closed loop control is implemented to achieve the exact predefined loads.

The ETW standard load schedule starts with single loads for all six balance components over the complete balance load range. The following numbers describe a standard calibration which can be adapted to special requirements if necessary. For each component, eight different loads are applied once during loading and repeated during unloading to check hysteresis effects. Including zero cases, this results in 17 measurement points. After the single factor loadings, loadings are conducted with two factors at a time. This combination results in an additional 70 measurement points per load combination resulting in a total number of 1152 calibration measurement points representing 528 different load cases of single and two-component loads. Figure 2 shows a schematic for a single load case and a combined load case.

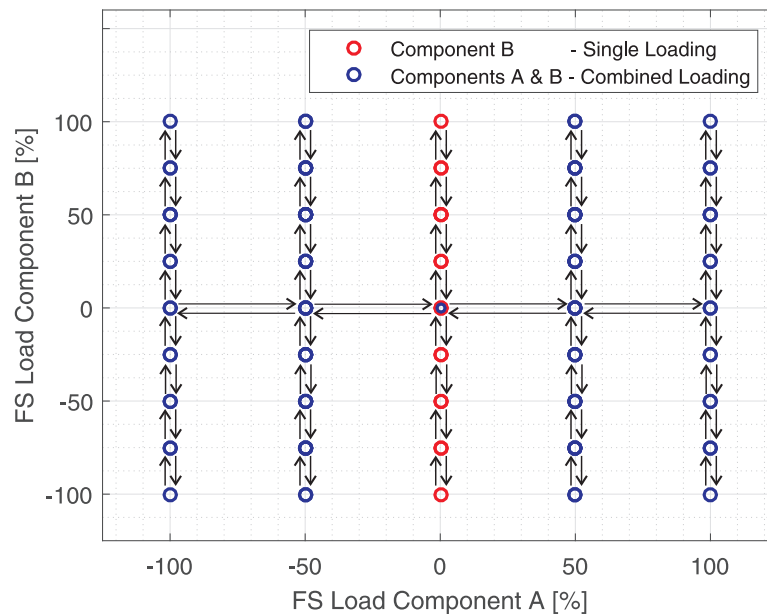


Figure 2. Default single and combined schedule used at ETW.

After the measurement of all calibration points, a regression technique is used to create a balance calibration matrix from the component bridge outputs and the loads applied and also the matrix from applied

loads to bridge outputs which is also required for data reduction purposes.

II.B. NASA's Approach

Figure 3 shows an example of a dead weight, long arm calibration method^{5,6} used for the room temperature calibration of cryogenic forces balances that are over 3,000 pounds of normal force in load carrying capacity. While the key hardware pieces are shown, readers are encouraged to consult the references for a more thorough explanation of the process.

As shown, the basis of the long arm process is the direct application of free weights. The three ways of applying free weight using the long arm process are highlighted in figure 3. Forces can be applied directly over moment center via hangers precisely positioned using knife edges. Moments are applied using a small fraction of the force transferred at a long distance via moment arms attached to the balance calibration fixture. To apply multiple forces simultaneously, a hanger assembly attached to a strap that is run over a bell crank is used.

To maintain known alignment of the forces generated by the weights, the balance is repositioned relative to gravity after each load application to compensate for deflection.

The calibration consists of 82 combinations of one and two component loads and several three and four-component loads to derive the calibration matrix. Several three component confirmation loads are performed and used as check loads to validate the effectiveness of the calibration matrix. The single component loads make up what is referred to as a primary calibration.

A regression technique is then used to estimate a balance calibration matrix from the component bridge outputs and the loads applied.

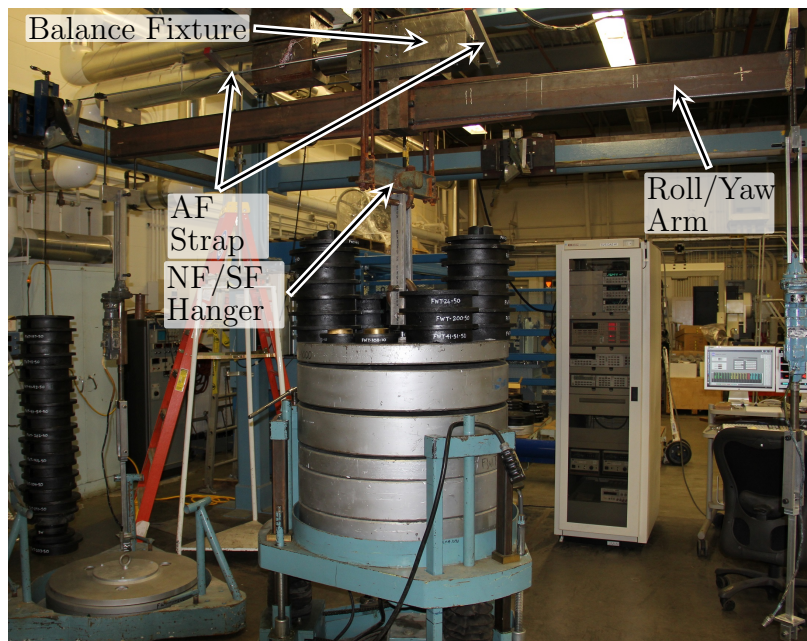


Figure 3. Example of hardware used for room temperature calibration at NASA.

III. Cryogenic Calibration Methods

Cryogenic calibration is necessary because the elastic modulus of the force balances changes with temperature and the gage factors of the strain gages installed on the force balances change with temperature.

The hardware and methodologies used to perform cryogenic calibration of force balances at NASA and ETW are different. In addition, the philosophies used to apply the corrections are different. For instance, ETW performs full calibrations at multiple temperatures and then uses the derived matrix corresponding to the temperature closest to the tunnel operating temperature. The NASA process uses a limited set of cryogenic loads to update the primary sensitivities of the calibration matrix. The following sections outline each of these approaches in more detail.

III.A. ETW's Approach

ETW's approach for cryogenic calibration is similar to the room temperature calibration. Using the cryogenic calibration chamber, the internal balance is conditioned to discrete temperatures and then calibrated following the procedure described in section II.A. Also, the loads and the number of calibration points are identical to the room temperature calibration. For a standard full calibration, the calibration temperature varies in steps of 25K in the range between 325K down to 200K and is then reduced for temperatures below 200K to a 10K calibration temperature interval. Including room temperature, this calibration approach contains full calibrations at 16 different temperature levels. A repeat calibration at ambient temperature is added.

For each temperature, a calibration matrix is calculated using a regression method. During testing in ETW at cryogenic temperatures, the calibrations matrix of the temperature closest to the actual mean balance temperature is selected and applied for data evaluation. No interpolation between matrices is performed for intermediate temperatures.

As an example, Figure 4 shows the change of the matrix sensitivities compared to ambient temperature of the main bridges influencing normal force and pitching moment for two different ETW balances. The B003 and B004 balances are N1, N2 type balances where two bridges are combined to form the normal and pitch components. Here, the N1 and N2 bridges are presented in matrix form such that $Z_{3,3}$ is the sensitivity change of the N1 bridge due to the application of normal force and $Z_{5,3}$ is the sensitivity change of the N2 bridge due to the application of normal force. $M_{3,5}$ and $M_{5,5}$ are the sensitivity changes of the N1 and N2 bridges with respect to pitching moment. The figure indicates that the change of sensitivities is strongly dependent on the balance itself, the temperature compensation of its bridges, and its temperature stability in general. Comparing the two balances shown, it is visible, that balance B003 (Figure 4 left) has a higher change in sensitivities than B004 (Figure 4 right), but shows a smoother characteristic with temperature than B004. Both sensitivity changes show a highly non-linear trend over temperature, so that for high accuracy demands these non-linear effects have to be taken into account.

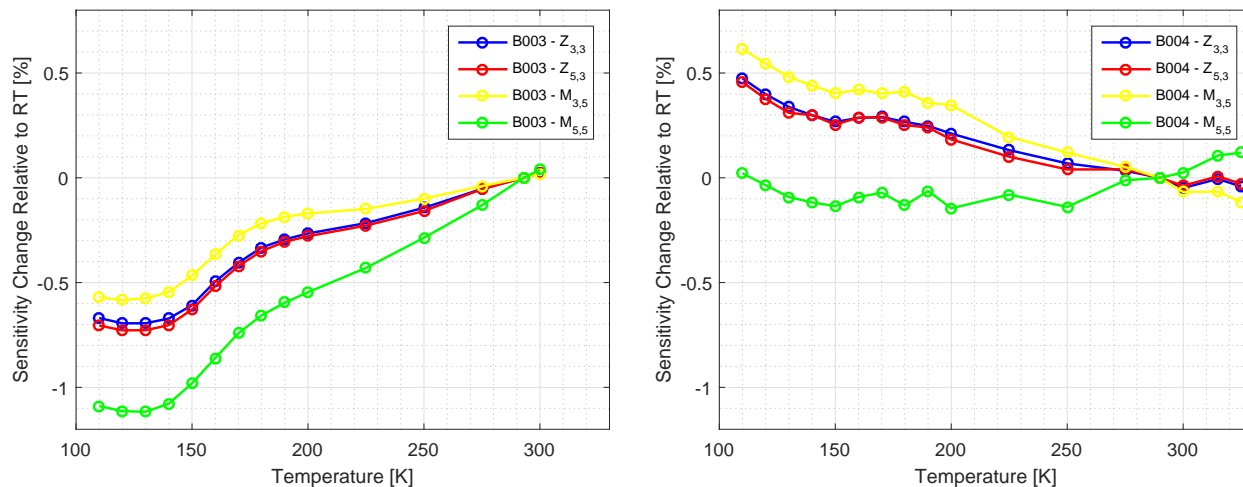


Figure 4. Change in ETW's B003 and B004 force balance sensitivities due to temperature changes.

III.B. NASA's Approach

III.B.1. Experimental Approach

Rather than a full cryogenic calibration, Langley augments the full room temperature calibration with primary cryogenic loads.⁷ The cryogenic loads are performed in a dedicated calibration fixture shown in Figure 5 that incorporates channels for liquid nitrogen to circulate through the fixture on the metric end and non-metric end.

A yoke attaches to the balance fixture (Figure 5) that is thermally isolated from the balance fixture to maintain ambient temperature of the calibration hardware beyond the fixture. It incorporates knife edge

grooves for the application of normal, side, and axial force via free hanging dead weight on hangers accurately placed using knife edges. Rolling, yawing, and pitching moments are applied by attaching long arms to the yoke and applying dead weights at the ends of the arms.

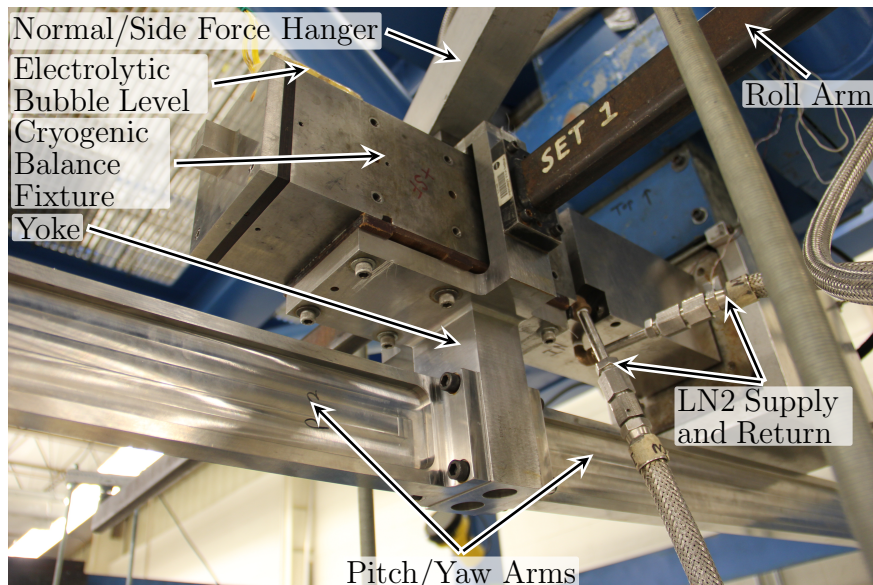


Figure 5. Hardware used for cryogenic calibration at NASA.

For a direct relative comparison using the cryogenic calibration hardware, calibration loads with the cryogenic hardware installed are performed at room temperature and approximately 88K. The relative difference between the bridges' output at 295K and 88 K is used for the thermal corrections. To infer behavior between 88K and 295K, linear interpolation is used.

As in the room temperature calibration, the balance fixture is re-leveled to accommodate for deflection using a heated electrolytic bubble level package.

A different set of hardware is used to determine the zero shift of the bridges' output as a function of temperature. This process does not involve the application of load, rather the temperature is lowered from 295K while recording the output of the bridges at 5 minute intervals. This temperature excursion is performed with the balance model block and the wind tunnel model installed on the balance.

III.B.2. Modeling Approach

The NASA modeling approach adjusts bridges' output at a given temperature back to the readings that would have been obtained at room temperature (295 K). Thus, in the NASA approach temperature effects are accounted for in the bridges' output. By adjusting the bridges' output at a given temperature back to room temperature, the full room temperature calibration matrix can then be used to predict applied loads.⁸ The following equations form the basis of this approach.

The factors contributing to the bridge output (V_T) under the application of load and at cryogenic temperatures can be represented as:

$$V_T = V_{EZ,295} + \Delta V_{EZ} + V_{load} \quad (1)$$

where $V_{EZ,295}$ is the bridge electrical zero at 295K, ΔV_{EZ} is the zero shift of the bridge output at a given temperature under constant load, and V_{load} is the bridge voltage due to model weight and applied aero loads at a given temperature.

Adjusting the zero shift of the bridge output as a function of temperature is done by performing a second order curve fit to the recorded data described in section III.B.1 producing an equation of the form:

$$\Delta V_{EZ} = C_0 + C_1 T + C_2 T^2 \quad (2)$$

where C_0 , C_1 , and C_2 are the temperature compensation coefficients derived from the curve fit and T is the temperature from the resistance temperature detector (RTD) closest to that bridge.⁸

V_{load} can further be represented as:

$$V_{load} = V_{load,295} * SC \quad (3)$$

where $V_{load,295}$ is the estimated bridge output at 295K based on the applied weight and aero loads, and SC is the temperature sensitivity constant determined from the applied cryogenic loadings described in section III.B.1. SC is itself a function of temperature and is defined as:

$$SC = 1 + SS(T - 295) \quad (4)$$

where T is the temperature in K and SS is the sensitivity change per degree change in temperature defined as:

$$SS = (B_T - B_{295}) / (B_{295} * (T - 295)) \quad (5)$$

where B_T is the full scale bridge output at cryogenic temperature T under applied load and B_{295} is the bridge output at $T = 295$ K under the same applied load.

Since the individual bridges are excited multiple times during the cryogenic primary loading sequence, an average of the SS coefficient from each of the loading sequences targeting that bridge is used in the determination of the SS coefficient.

Combining equations 1 and 3 above and solving for $V_{load,295}$:

$$V_{load,295} = (V_T - V_{EZ,295} - \Delta V_{EZ}) / SC \quad (6)$$

This equation is used to estimate the absolute bridge output due to applied model weight and aero loads at 295K based on the bridge output at the test temperature. These bridge outputs are then combined to form component outputs which can be used with the full room temperature calibration to estimate the applied loads on the balance.

IV. Simulation of Calibration Effects on Tunnel Results

An analysis, performed by NASA Langley force measurement engineers, was conducted to assess the plausibility of balance thermal correction errors being responsible for the discrepancy in wind tunnel results. This analysis shows how the calibrations and methodologies described in section III are applied to the raw bridge signals recorded during the wind tunnel test. Hypothetical changes to the thermal corrections are made to evaluate their effects on the wind tunnel results.

IV.A. Analysis

The analysis sought to go from the raw bridge outputs from NTF Test 197, Run 220 and walk through the steps required to generate aerodynamic data. First, the electrical zero shift was calculated for each bridge, according to equation 2, based on the temperature reading from the closest RTD to the bridge. The temperature sensitivity constant, SC , was then calculated for each bridge using equation 4 and the temperature reading from the closest RTD to the bridge. The bridge outputs were then adjusted back to 295 K, using equation 6. At this point, the bridge outputs (i.e. N1, N2) were combined to form components (i.e. NF) according to the force balance wiring specifications. The calibration matrix determined from the full room temperature calibration was then used to calculate the applied load for each component.

Discrepancies between normal force and pitching moment polars for NTF test 197, run 220 and ETW test 0001, run 232 appeared to be at constant offsets relative to angle of attack.² Utilizing information available for the fluid dynamic pressure, surface area of the model, and reference chord length, these curve offsets correspond to normal force and pitching moments offsets of 120 lbs and 156 in-lbs respectively. For perspective, these offsets are approximately 1.8% of the NTF-118A's full scale normal force load range and 1.2% of the full scale pitch load range. In the subsequent plots, unaltered NTF data is used as a baseline and ETW reference data is simulated by applying the observed normal force and pitching moment offsets to the NTF baseline.

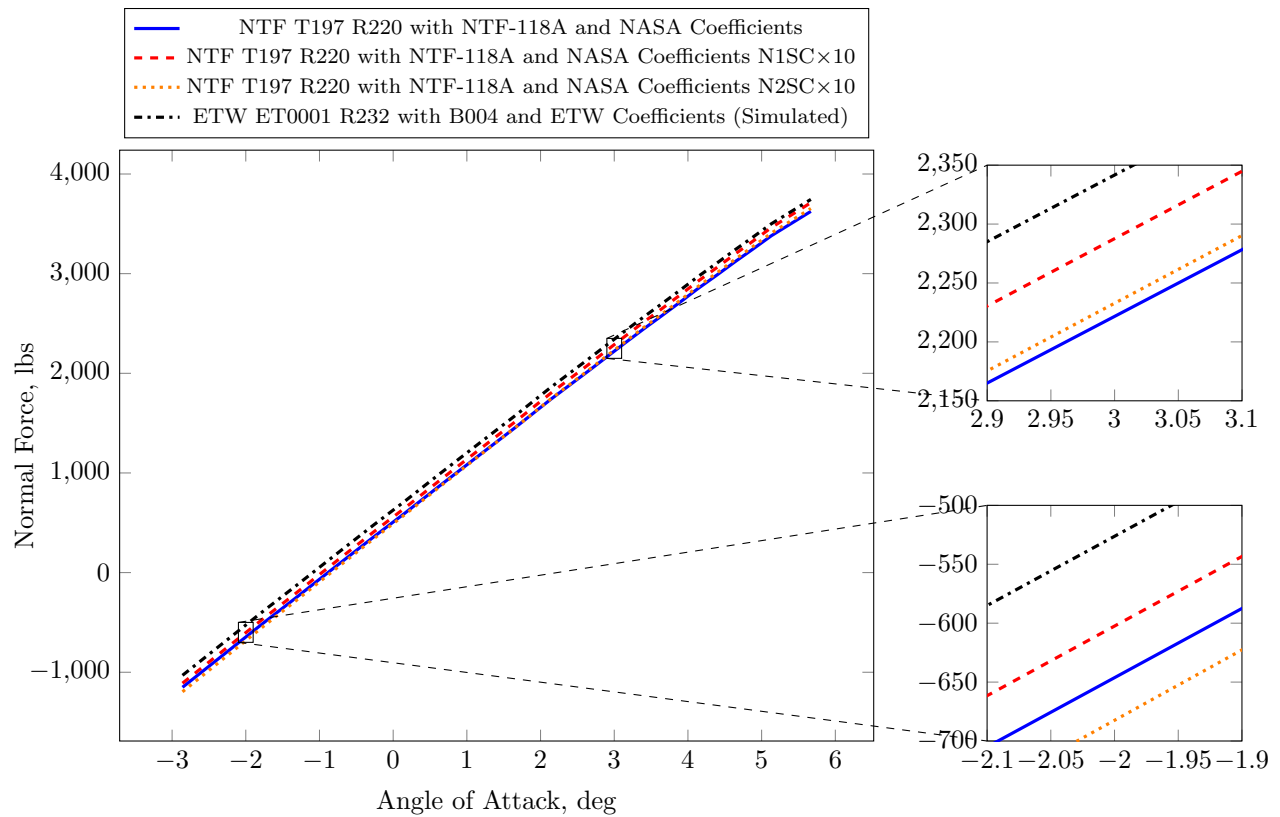


Figure 6. Effects of SCs on measured normal force.

The effects of varying the cryogenic sensitivity constants (SCs) are illustrated in Figure 6. Here, the N1 and N2 cryogenic SCs have been independently multiplied by 10 before being combined to form normal force and pitching moment. By comparing these curves to the baseline curve, it is clear that changes to the cryogenic SCs have an influence on the slope of the curve. This is consistent with what is expected given that based on Equation 6 the effective room temperature output is directly proportional to the cryogenic SCs. This change in slope will not reconcile the fixed offset behavior seen in the NTF and ETW lift and pitch coefficient curves. Moreover, the large SC multiplier of 10 (suggesting SC measurements are off by an order of magnitude) required to generate observable differences in the normal force polar suggests that this is an impractical explanation for the NTF and ETW tunnel discrepancies.

V. Room Temperature Calibration Results

Room temperature calibrations of the NTF-118A were performed at NASA and ETW as outlined in section III.B.1. A second order matrix (6x27) was generated from the NASA and ETW calibrations and the percent difference of the full scale effect of each interaction in the matrix was computed. The differences are shown in a bar chart (Figure 7), where the magnitude of the ETW coefficients has been subtracted from the NASA coefficients.

From this figure, it is clear that there is generally good agreement between the vast majority of the terms in the two matrices. The most significant exception to this is the term associated with applying normal force while measuring axial force. Here, the difference in the magnitude of the two coefficients is 0.55%, which corresponds to a difference in predicted axial force of 3.9 lbf with the full application of 6520 lbf of normal force.

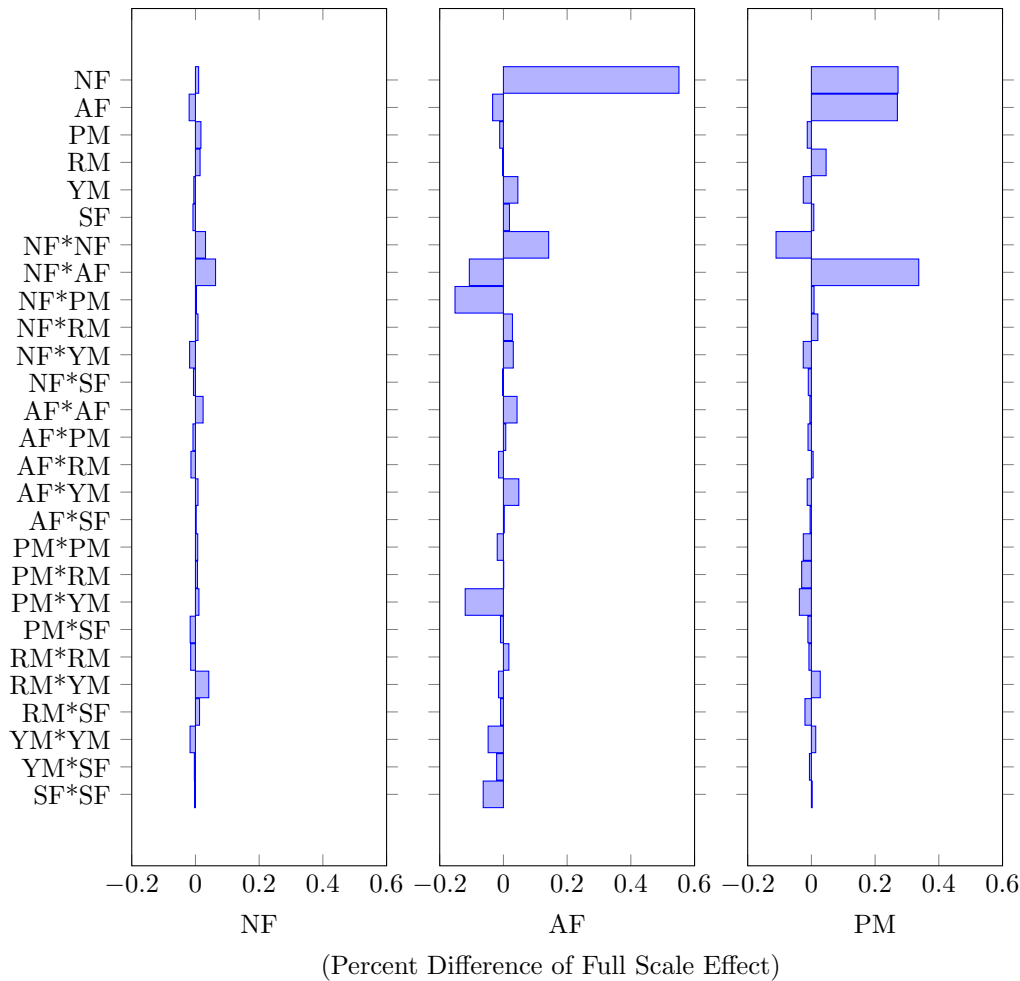


Figure 7. Room temperature differences between NASA and ETW calibrations.

VI. Cryogenic Calibration Results

Comparison of the cryogenic calibration results must consider differences in the calibration processes. The only complete calibration performed at NASA is at room temperature preventing the direct comparison of full calibration matrices at other temperatures. Moreover, ETW's automatic calibration machine does not routinely apply pure single component loads, rather a primary component is applied and residual loads remain on the other five components. This prevents the direct use of the ETW data via the NASA approach, which relies on pure single component loads to estimate the sensitivity change with temperature (Equation 5).

Therefore, a comparison using the NASA approach was performed where the thermal sensitivity corrections were estimated by using regression to calculate the effective coefficients from the ETW dataset. In this method, a full 6x27 calibration matrix was estimated for each of the discrete temperatures that ETW conducted a calibration of the NTF-118A. Whereas, the NASA approach utilized equation 5, but exchanged the bridge outputs with component outputs to be consistent with the ETW regression results.

Figure 8 shows how the normal force primary sensitivity varies with temperature for the NTF-118A as a percent of the NASA room temperature sensitivity. The measured sensitivity changes are shown for the NASA and ETW calibrations. In the figure, a line was fit to the two NASA datapoints (at 295K and 88K) as a linear interpolation between these two points to determine the sensitivity constant at a given temperature. A quadratic fit the ETW datapoints was used. Note that an additional NASA data point was taken at an intermediate temperature of 144K. It appears to be in relative agreement with the ETW data but was not included in the line fit, since the typical procedure only uses data points at 295K and 88K.

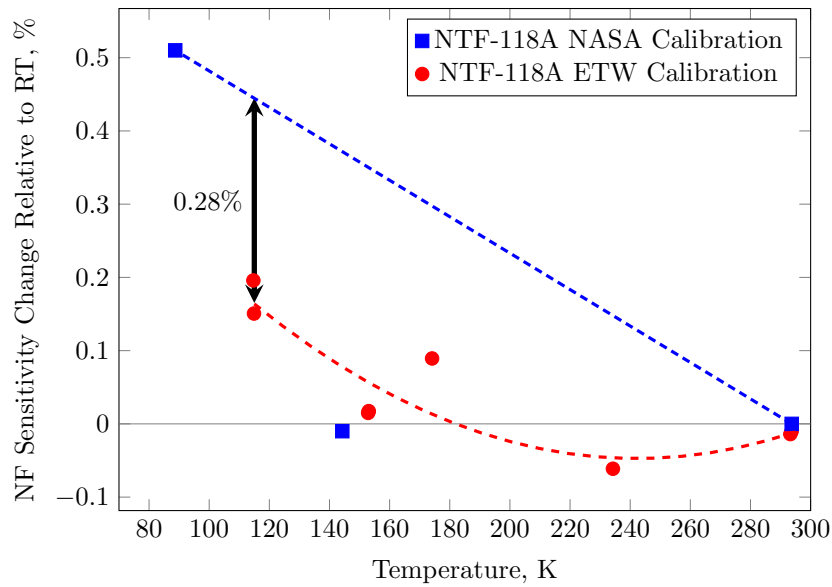


Figure 8. NTF-118A normal force sensitivity change relative to room temperature sensitivity.

From Figure 8, a 0.28% difference exists between the normal force sensitivity change measured by NASA and ETW at 116K where the wind tunnel discrepancy was observed. This difference is significant relative to the stated balance accuracy and suggests that the NASA approach may need to reconsider the linear interpolation assumption for this combination of balance material and strain gages.

Figure 9 shows how the axial force primary sensitivity varies with temperature for the NTF-118A as a percent of the NASA room temperature sensitivity. The measured sensitivity changes are shown for the NASA and ETW calibrations. The sensitivity changes measured by NASA and ETW are in good agreement. It is also clear that a quadratic fit to the data may be more appropriate than a linear fit. The axial sensitivity change relative to room temperature is observed to be larger than the normal sensitivity change. A different gaging strategy used on the axial force bridge likely explains this observation.

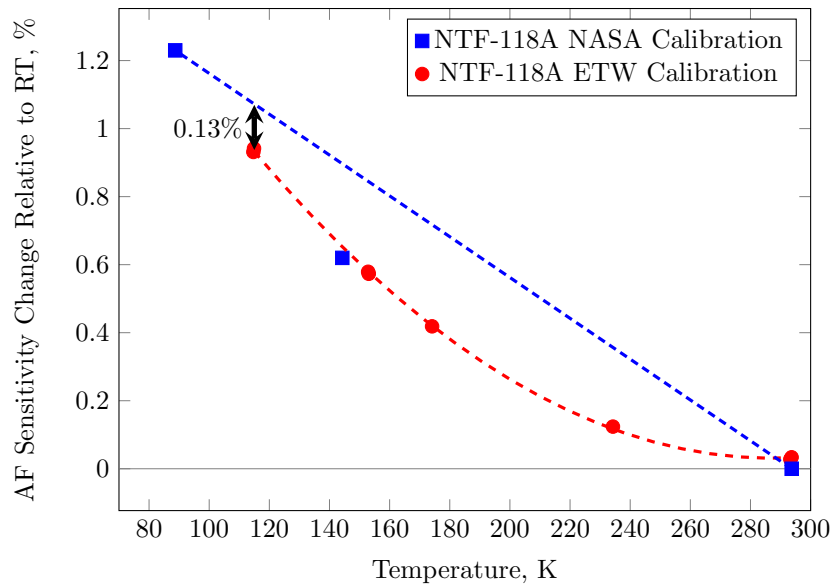


Figure 9. NTF-118A axial force sensitivity change relative to room temperature sensitivity.

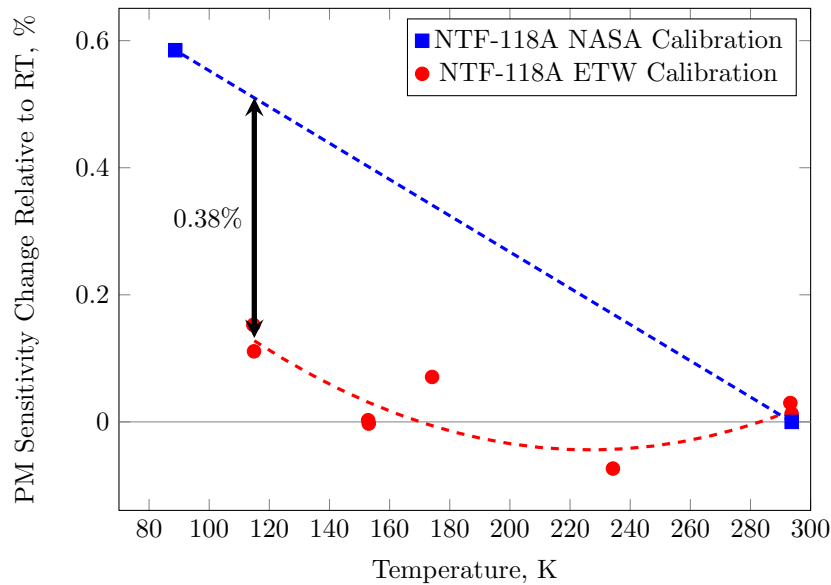


Figure 10. NTF-118A pitching moment sensitivity change relative to room temperature sensitivity.

Figure 10 shows how the pitching moment primary sensitivity varies with temperature for the NTF-118A as a percent of NASA’s room temperature sensitivity. The measured sensitivity changes are shown for the NASA and ETW calibrations. From the figure, the ETW data suggests that a quadratic fit to the data is most appropriate. The lack of intermediate points and the linearity assumption for the NASA data leads to a 0.38% difference in the measured pitching moment sensitivity change at 116K.

VII. Influence of Calibrations on Wind Tunnel Results

The main objective of this effort was to explore whether errors in the balance thermal corrections could account for discrepancies between the wind tunnel results. This section applies the NTF-118A balance calibrations performed at NASA and ETW using each facilities calibration approach to the raw bridge outputs from NTF test 197, run 220 to determine the influence of the calibrations on the NTF wind tunnel results.

Figure 11 shows three curves of the normal force exerted on the CRM model as a function of the angle of attack of the model. The solid blue line is the normal force exerted on the CRM using the NASA calibration of the NTF-118A and coefficients as outlined in sections II.B and III.B. The red dotted line is the normal force exerted on the CRM based on the calibration of the NTF-118A at ETW and the derived coefficients as outlined in sections II.A and III.A. Finally, the black dotted line is an estimate (assuming a 120 lb offset from the blue line as discussed in IV.A) of the ETW test 0001, run 232 normal force loads using the ETW B004 balance and ETW derived coefficients.

From this figure, the calibration performed at ETW of the NTF-118A does not reconcile the NTF test 197, run 220 and ETW test 0001, run 232 differences. It is also clear that the differences between the two calibrations (and resultant matrices) are not generating the vertical offset behavior required to reconcile the two tunnel entries. Rather, the difference in calibrations is resulting in a slight rotation of the curves with respect to one another. However, this slight rotation of the blue and red curves with respect to one another is insignificant with respect to the NTF test 197, run 220 and ETW test 0001, run 232 differences.

Similar to the normal force observations, Figure 12 shows three curves of the pitching moment exerted on the CRM model as a function of the angle of attack of the model. Here, the solid blue line is the pitching moment exerted on the CRM using the NASA calibration of the NTF-118A and coefficients. The red dotted line is the pitching moment exerted on the CRM based on the calibration of the NTF-118A at ETW and the derived coefficients. Finally, the black dotted line is an estimate (assuming a -156 lbs offset from the blue line as discussed in IV.A) of the ETW test 0001, run 232 pitching moment loads using the ETW B004 balance and ETW derived coefficients.

The results again show that the differences in the measured sensitivities from the NASA and ETW

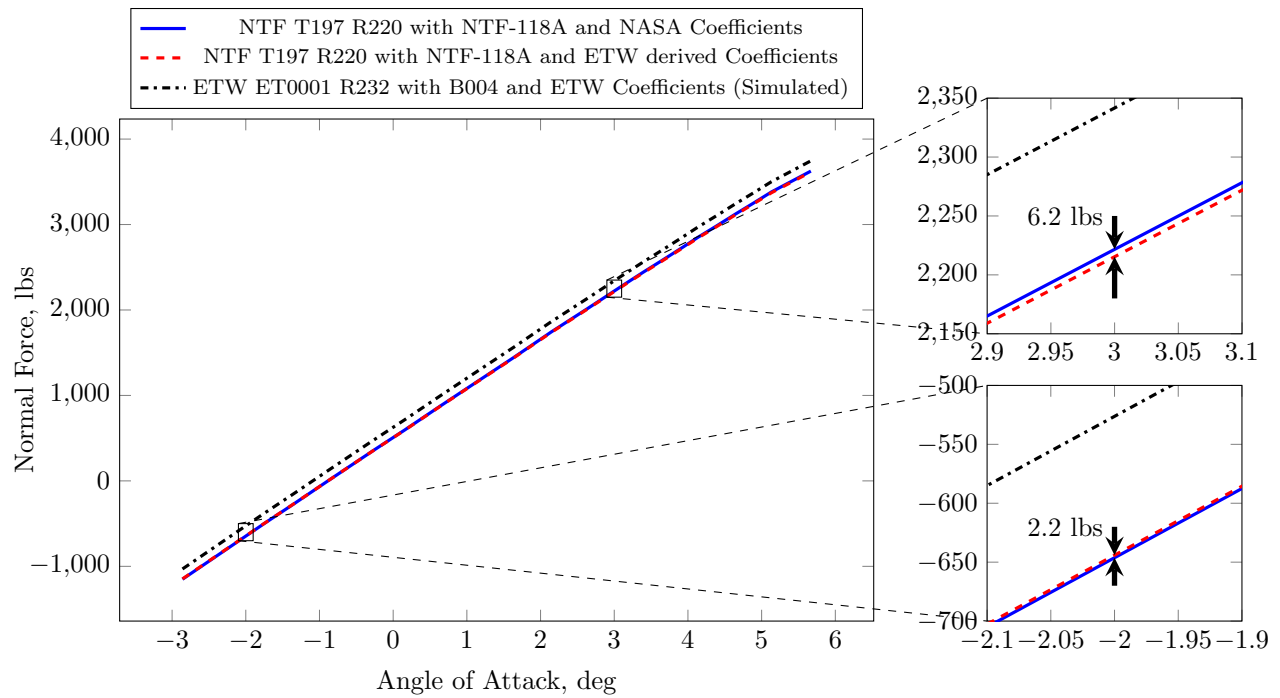


Figure 11. Effects of calibrations on measured normal force with respect to NTF and ETW tunnel entries.

calibrations result in a slight rotation of the predicted NTF test 197, Run 220 pitch polars. However, this slight rotation is insignificant with respect to the tunnel differences.

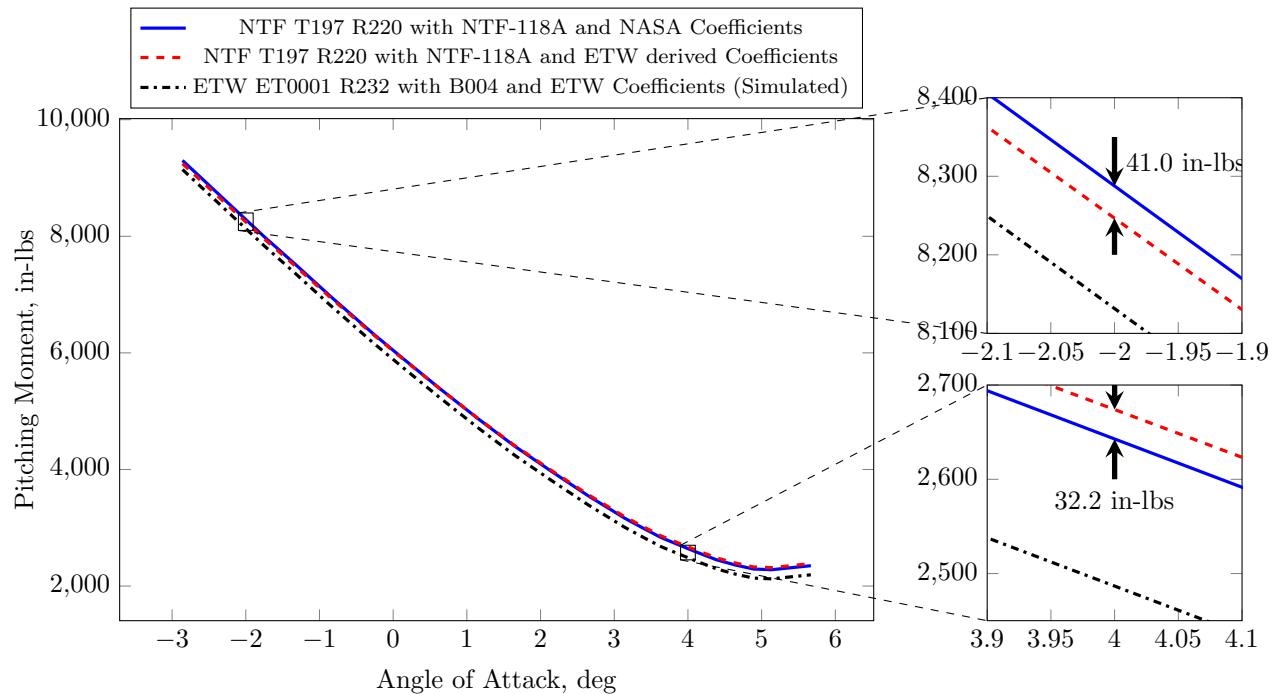


Figure 12. Effects of calibrations on measured pitching moment with respect to NTF and ETW tunnel entries.

VIII. Conclusions

This work sought to determine whether differences in the ETW and NASA force balance thermal compensation of the sensitivity change as a function of temperature could be responsible for discrepancies observed during independent entries at ETW and NTF of the CRM at high Reynolds numbers and low temperatures. Simulation studies showed that balance thermal corrections were unlikely to explain the wind tunnel discrepancies observed. This was confirmed by comparing calibrations of the NTF-118A balance at NTF and ETW. While some differences between the calibrations were observed, these differences were insignificant with respect to the wind tunnel discrepancies.

This joint calibration exercise provided valuable intermediate temperature data to NASA personnel. It showed that historical assumptions regarding the linearity of the thermal sensitivity constants could be reconsidered, particularly when it comes to the NTF-118A balance material.

While NASA and ETW take two different strategies towards calibration and use two different cryogenic calibration systems, both approaches produce results that are within acceptable wind tunnel tolerance levels. This is encouraging given the extent of the differences between the approaches and should provide continued confidence in the use of these balances and methods at cryogenic temperatures.

References

- ¹Rivers, M. and Dittberner, A., "Experimental Investigations of the NASA Common Research Model (Invited)," Fluid Dynamics and Co-located Conferences, American Institute of Aeronautics and Astronautics, June 2010.
- ²Rivers, M. B., Rudnik, R., and Quest, J., "Comparison of the NASA Common Research Model European Transonic Wind Tunnel Test Data to NASA Test Data (Invited)," AIAA SciTech Forum, American Institute of Aeronautics and Astronautics, Jan. 2015.
- ³POLANSKY, L., "A new and working automatic calibration machine for wind tunnel internal force balances," Joint Propulsion Conferences, American Institute of Aeronautics and Astronautics, June 1993.
- ⁴Mantik, J., Quix, H., Struddthoff, W., Jansen, U., and Ernst, F., "Modification of the Control & Measurement Software for the Balance Calibration Machine at ETW," 9th International Force Balance Symposium, 2014.
- ⁵Ferris, A. J., "Strain Gauge Balance Calibration and Data Reduction at NASA Langley Research Center," *First International Symposium on Strain Gauge Balances*, NASA / CP-1999-209101 / PT2, 1999, pp. 565-572.
- ⁶Gaurino, J. F., "Calibration and Evaluation of Multicomponent Strain-Gage Balances," NASA Interlaboratory Force Measurements Group Meeting, JPL, 1964.
- ⁷Parker, P., "Cryogenic balance technology at the National Transonic Facility," Aerospace Sciences Meetings, American Institute of Aeronautics and Astronautics, Jan. 2001.
- ⁸Foster, J. M. and Adcock, J. B., "User's Guide for the National Transonic Facility Research Data System," Technical Memorandum 110242, National Aeronautics and Space Administration, Langley Research Center, Hampton, Virginia 23681-0001, April 1996.